

Geometric Control of Manganese Redox State

Michael G. B. Drew,^c Charles J. Harding,^b Vickie McKee,^a Grace G. Morgan^{a,b} and Jane Nelson^{a,b}

^a School of Chemistry, Queens University, Belfast, UK BT9 5AG

^b Department of Chemistry, Open University, Milton Keynes, UK MK7 6AA

^c Department of Chemistry, University of Reading, UK RG6 2AD

Comparison of the structures of four monomanganese (and one monoiron) complexes of ligands with the identical donor $[N_3(O^-)_3]$ set reveals that geometry determines the redox state of the cation.

The geometric preferences which contribute to the stability of different oxidation states of copper in bioinorganic chemistry¹ are widely accepted and well understood, to some extent because the numerous cuproprotein crystal structures which have been obtained emphasise the validity of the correlations. Although the mechanism of control of manganese redox states is of equally vital concern, a similar understanding has not developed in this case, perhaps because of the scarcity of information on manganese biosites. It seems probable, however, that the non-redox functions of manganese in biology rely on geometry, among other things, to restrict access to potentially hazardous higher oxidation states. On the other hand, where redox function is involved, geometry may again be exploited, this time to enable easy access to oxidation states higher than II.

The geometric requirements of specific manganese redox states in small molecule models have not so far been extensively studied; there is² no reliable basis for predicting the circumstances under which a particular donor set will stabilize the II, III or IV states of manganese. Coordination number effects (which cannot be separated from geometry) have been invoked as the origin of different redox state stabilisations.³ While in acyclic or macrocyclic situations, it can be difficult to rule out hemicoordination of counterion or solvent accompanying alteration of ligand geometry, cryptand ligands offer a coordination number-invariant environment, and have the further advantage of diminishing any tendency to decomplexation in solution, so that structural information obtained in the solid state can be applied validly to the interpretation of solution properties.

The cryptands L^1 (ref. 4) and L^2 (ref. 5) designed for the complexation of +3 oxidation state cations of Group 13 and lanthanoids,⁵ can act as mononucleating ligands providing three

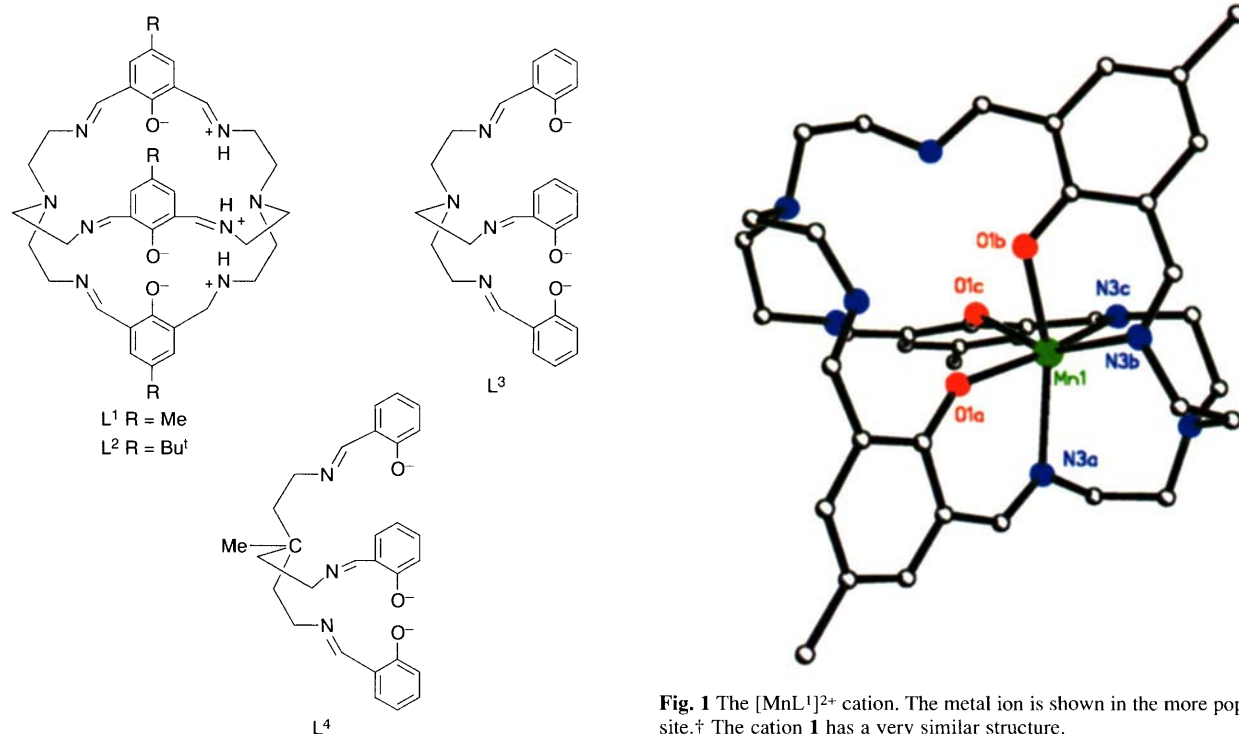


Fig. 1 The $[MnL^1]^{2+}$ cation. The metal ion is shown in the more populated site.[†] The cation **1** has a very similar structure.

Table 1 Magnetic and EPR spectroscopic properties of the cryptand and podand complexes

Compound	magnetic moment/ μ_B		<i>g</i> -Values	EPR Parameters	
	80 K	300 K			
1 $[FeL^1][ClO_4]_3 \cdot 0.5MeCN$	4.05	4.05	2.00, w, br ^a	4.20, br ^a	6.20, br ^a
2 $[FeL^2][ClO_4]_3$	3.21	3.58	2.05, w, br ^a	4.10, br ^a	6.30, br ^a
3 $[MnL^1][BPh_4]_2$	5.7 ^f	5.9 ^f		2.02 ^b (100 G ^c)	
4 $[MnL^2][ClO_4]_2$	5.9	5.9		1.98 ^b (88 G ^c)	
5 $[MnL^3] \cdot 0.5H_2O$	4.63	4.82		^e	
6 $[MnL^4]ClO_4$	3.82	3.81	1.97, br ^{a,d}	3.89, br ^a	

^a Polycrystalline, 113 K. ^b g_{iso} DMF glass, 113 K. ^c A_{iso} , DMF glass, 113 K. ^d Poorly resolved, 80 G, hyperfine. ^e No polycrystalline EPR observed. ^f Magnetic measurements run on BF_4^- salt.

locally anionic phenolate (via proton transfer from phenol to imine nitrogens: see **L**¹ structure) and three imino-N donors from one end of the cryptand. The preference of these ligands for M³⁺ cations may be expected to extend to the first transition series, so we anticipated ready isolation of iron(III) and manganese(III) cryptates. Transmetalation of NaL¹ or NaL²

with Fe^{II} or Fe^{III} salts under aerobic conditions does generate the mono-Fe^{III} product. Magnetic and spectroscopic data (Table 1) indicate distortion from regular octahedral geometry, which is sufficient to generate a spin-quartet ground state for the perchlorate salt [FeL¹][ClO₄]₃ **1** and more complex low-spin magnetic behaviour⁶ for [FeL²][ClO₄]₃ **2**. X-Ray crystallo-

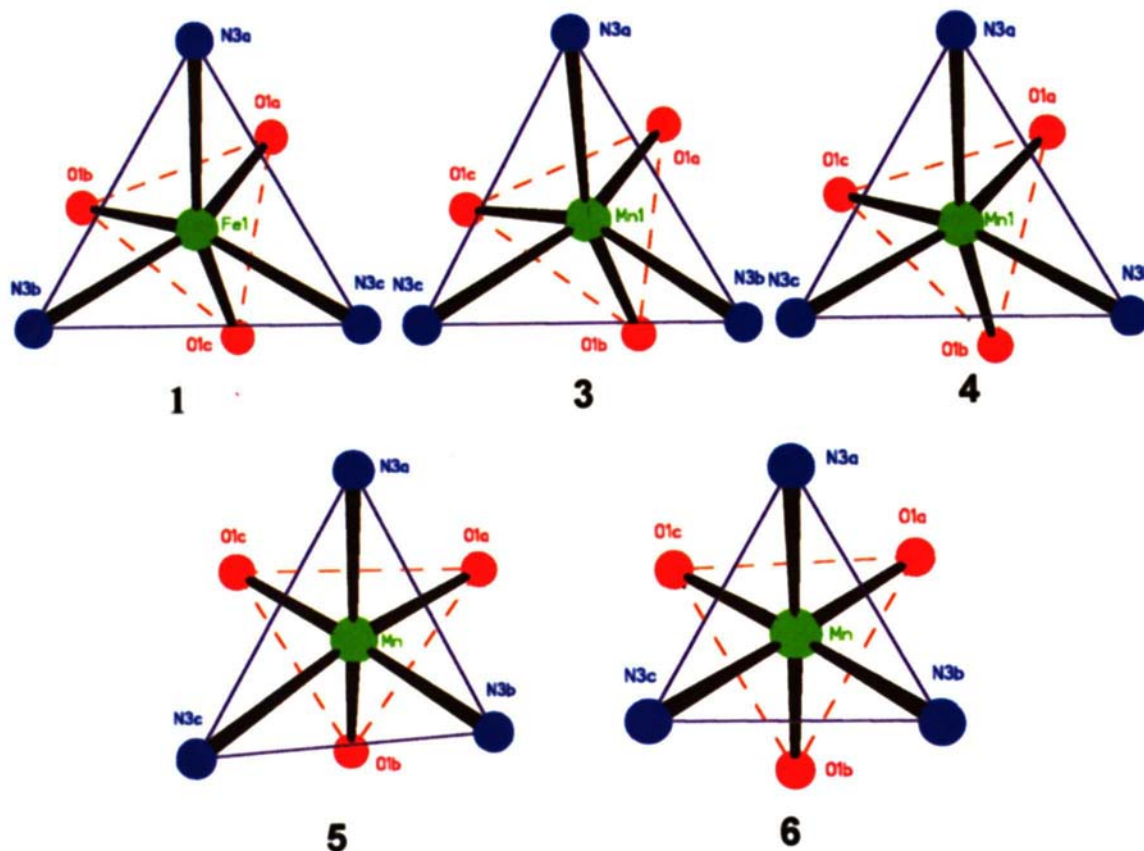


Fig. 2 The coordination geometries of **1**, **3**, **4**, **5** and **6** viewed perpendicular to the plane of the three nitrogen donors

Table 2 Geometric data

	1 Fe ^{III} <i>R</i> $\bar{3}$	3 Mn ^{II} <i>P</i> $\bar{1}$	4 Mn ^{II} <i>P</i> 2 ₁ / <i>n</i>	5 Mn ^{III} <i>P</i> 2 ₁ / <i>n</i>	6 Mn ^{IV} <i>C</i> <i>c</i>
M–O/Å	2.039(7)	2.029(5) 2.101(4) 2.194(4)	2.133(7) 2.135(8) 2.294(9)	1.893(3) 1.902(3) 2.117(4)	1.853(2) 1.868(1) 1.881(2)
M–N/Å	2.343(8)	2.332(5) 2.356(5) 2.419(6)	2.256(9) 2.294(8) 2.294(9)	2.051(4) 2.083(4) 2.327(4)	1.985(2) 1.995(2) 1.997(2)
Σ (dev. from 90°) ^a	140	129	123	59	20
O···O/Å	2.71	2.80 2.81 2.83	2.76 2.78 2.79	2.67 2.77 3.02	2.62 2.68 2.72
N···N/Å	3.75	3.57 3.64 3.75	3.55 3.60 3.63	3.13 3.15 3.45	2.72 2.73 2.77
Interplanar distance/Å ^b	2.22	2.42	2.37	2.18	2.26
Interplanar angle/ ^o ^b	0	3	2	8	1
Twist angle, φ / ^o ^c	40.3	36.0 38.4 39.3	43.5 44.9 45.2	61.5 62.0 64.1	58.3 58.8 59.5

^a Sum of the deviation from 90° of the 12 *cis* angles in the coordination sphere. ^b Between the N₃ and O₃ planes. ^c Projected angle between the N₃ and O₃ triangles.

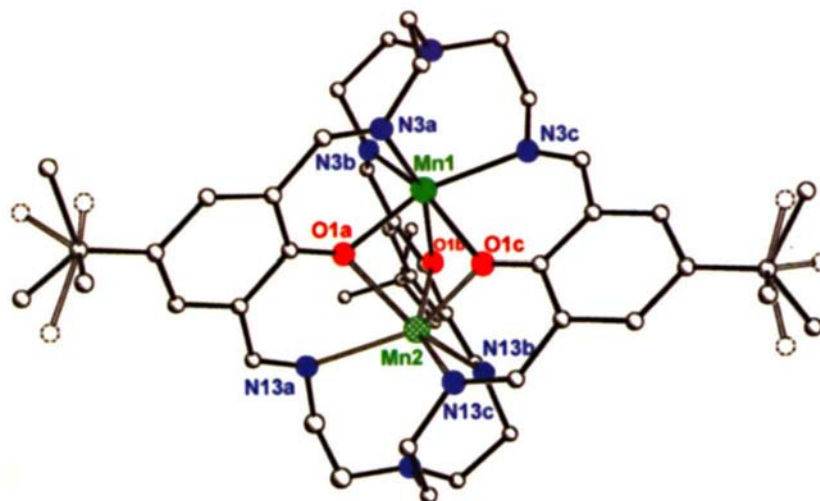


Fig. 3 Structure of $[\text{MnL}^2]^{2+}$; the solid and hatched green circles correspond respectively to major and minor positions for Mn^{2+}

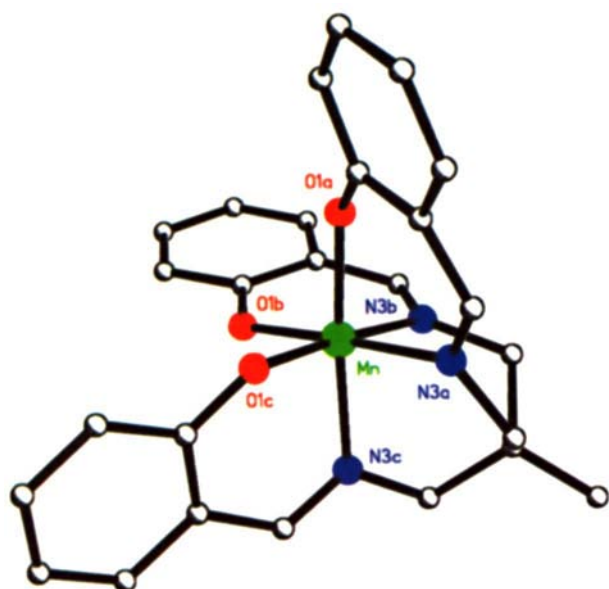


Fig. 4 The $[\text{MnL}^4]^+$ cation†

graphic structure determination of **1** confirms distortion of octahedral coordination geometry towards a trigonal prismatic arrangement (Fig. 1). The twist angle^{7,8} (Fig. 2, Table 2), $\varphi = 40.3^\circ$, is intermediate between that expected for trigonal prismatic (0°) and trigonal antiprismatic (60°) geometries.

The monomanganese cryptates, on the other hand, whether synthesised by transmetallation of the sodium templates with Mn^{II} or Mn^{III} , are obtained in the Mn^{II} state. Their coordination geometry (Figs. 1–3, Table 2) is similar to that of the Fe^{III} analogues, with somewhat less distortion in the L^2 cryptate ($\varphi_{\text{av}} = 44.5^\circ$ for **4** vs. 37.9° for **3**). In all three structures the Mn–N distances are considerably longer than the Mn–O bonds.

The trigonal distortion revealed in the crystal structures of **1**, **3** and **4** is acceptable to the d^5 cations, Fe^{III} and Mn^{II} , while the reduced Fe^{II} (d^6) or oxidised Mn^{III} (d^4) states have more specific geometric requirements which cannot easily be met within the rigid cryptand framework. Where a ligand with the same donor set lacks the built-in rigidity of the cryptand, no trigonal distortion is enforced, and square-based octahedral or tetragonal sites may be achievable. The podands L^3 (refs. 9 and 10) or L^4 (ref. 10) fall into this class, having an identical $[\text{N}_3(\text{O}^-)_3]$ donor set (3 imino-N; 3 anionic phenolate- O^-). Template synthesis of L^3 and L^4 on Mn^{II} generates, respectively, the Mn^{3+} and Mn^{4+} complexes^{9,10} **5** and **6**. The stability of the III state in **5** and IV

state in **6** are illustrated by the relatively small values of the redox potentials (at -290 mV for II/III in **5**⁹ and 310 mV for III/IV for **6**,¹¹ vs. SCE). Fig. 3 illustrates the structure of **6** and that of **5** is broadly similar; coordination geometries are compared in Fig. 2 and Table 2. In both these structures, the twist angle φ is very close to 60° and angles at Mn are close to 90° . The expected Jahn–Teller tetragonal distortion is evident in **5**; such a tetragonal distortion is not required for Mn^{IV} , and **6** has a regular, almost octahedral, structure. Stabilisation of Mn^{IV} in a tripodant macrocyclic ligand has been ascribed to a similarly regular structure.^{8b} Given the identical donor set across the series of ligands L^1 – L^4 , we must attribute any alteration of redox preference to subtle but effective geometric factors. The similarity of coordination geometry in **1**, **3** and **4** shows that the cryptand hosts are restricted to trigonally distorted octahedral coordination geometry, which can readily accommodate d^5 cations but not the d^4 cation Mn^{III} . The more flexible podand ligand, L^3 , can provide the tetragonal geometry preferred by Mn^{III} , while steric restrictions in the smaller N_3 cap of L^4 enforce Mn–L dimensions appropriate to Mn^{IV} .

The existence of III and IV states of manganese¹² in the S_1 state of the water-oxidising complex of photosystem II suggests that both tetragonally distorted and more regular octahedral coordination sites are available in this resting state; it is tempting to speculate that photochemical rearrangements in the course of the catalytic cycle may involve (at least transient) alterations of site geometry.

We thank SERC for access to FAB-MS service (Swansea) and, together with the University of Reading, for funds for the Image Plate System; also the Open University Research Committee for support (to G. M.). We are grateful to Mr A. Johans for assistance with collection of crystallographic data,[†] and to Ms Nola McLernon for carrying out some of the cryptate syntheses as part of an undergraduate project.

Received, 19th January 1995; Com. 5/00338E

Footnote

† Crystal data for **1**: $[\text{FeL}^1]^{3+} \cdot 3\text{ClO}_4^- \cdot 0.5\text{MeCN}$, $\text{C}_{40}\text{H}_{49.5}\text{Cl}_3\text{FeN}_{8.5}\text{O}_{15}$, rhombohedral, space group $R\bar{3}$, $a = 15.803(7)$, $c = 30.703(11)$ Å, $U = 6640(3)$ Å³, $Z = 6$, $\mu = 0.60$ mm⁻¹, $F(000) = 3276$, 7426 Reflections ($6.5 < 2\theta < 52^\circ$), 2896 independent ($R_{\text{int}} = 0.066$), $wR2 = 0.365$, $\text{GoF} = 0.909$ (all data), conventional $R1 = 0.085$ ($I > 2\sigma I$). Fe Disordered over two sites with occupancies 0.60 and 0.40. For **3**: $[\text{MnL}^1]^{2+} \cdot 2\text{BPh}_4^-$,

$C_{87}H_{88}B_2MnN_8O_3$, triclinic, space group $P\bar{1}$, $a = 15.107(3)$, $b = 15.166(3)$, $c = 18.551(3)$ Å, $\alpha = 74.70(1)$, $\beta = 75.06(1)$, $\gamma = 64.14(1)^\circ$, $U = 3639(1)$ Å³, $Z = 2$, $\mu = 0.239$ mm⁻¹, $F(000) = 1450$. 9725 Reflections ($4 < 2\theta < 45^\circ$), 9294 independent ($R_{int} = 0.039$). $wR2 = 0.169$, GoF = 0.886 (all data), conventional $R1 = 0.065$ ($I > 2\sigma I$). Mn Disordered over two sites with occupancies 0.55 and 0.45. For **4**: $[MnL^2]^{2+} 2ClO_4^-$, $C_{48}H_{66}Cl_2MnN_8O_{11}$, monoclinic, space group $P2_1/n$, $a = 14.213(7)$, $b = 17.899(8)$, $c = 20.992(9)$ Å, $\beta = 92.86(1)^\circ$, $U = 5334(4)$ Å³, $Z = 4$, $\mu = 0.22$ mm⁻¹, $F(000) = 2172$. 16782 Reflections ($6 < 2\theta < 50^\circ$), 8722 independent ($R_{int} = 0.0798$). $wR2 = 0.298$, GoF = 1.156 (all data), conventional $R1 = 0.095$ ($I > 2\sigma I$). Mn Disordered over two sites with occupancies 0.78 and 0.22, two of the *tert*-butyl groups and both perchlorates were also disordered. For **5**: $[MnL^3] \cdot MeOH$, $C_{28}H_{31}MnN_2O_4$, monoclinic, space group $P2_1/n$, $a = 10.790(3)$, $b = 14.742(3)$, $c = 16.252(4)$ Å, $\beta = 94.98(2)^\circ$, $U = 2575(1)$ Å³, $Z = 4$, $\mu = 0.554$ mm⁻¹, $F(000) = 1136$. 3135 Independent reflections ($4 < 2\theta < 45^\circ$). $wR2 = 0.126$, GoF = 0.999 (all data), conventional $R1 = 0.053$ ($I > 2\sigma I$). For **6**: $[MnL^4]^+ ClO_4^-$, $C_{26}H_{24}ClMnN_3O_7$, monoclinic, space group Cc , $a = 14.049(3)$, $b = 25.495(5)$, $c = 9.645(2)$ Å, $\beta = 131.2(2)^\circ$, $U = 2594.9(9)$ Å³, $Z = 4$, $\mu = 0.663$ mm⁻¹, $F(000) = 1196$. 3147 Independent reflections ($4 < 2\theta < 45^\circ$). $wR2 = 0.066$, GoF = 1.101 (all data), conventional $R1 = 0.027$ ($I > 2\sigma I$). Refined as a racemic twin.

The data sets were collected using Mo-K α radiation ($\lambda = 0.71073$), **1**, **3** and **4** at room temp., **5** and **6** at 168 and 123 K, respectively. Empirical absorption corrections were applied to **3**, **5** and **6**. **5** was solved using a Patterson calculation, the others were solved by direct methods.¹³ Each structure was refined on F^2 using all the data.¹⁴ Non-hydrogen atoms were refined anisotropically and hydrogen atoms were inserted at calculated positions except for those on the imine nitrogen atoms in the cryptates, which were not included. Atomic coordinates, bond lengths and angles, and

thermal parameters have been deposited at the Cambridge Crystallographic Data Centre. See Information for Authors, Issue No. 1.

References

- 1 J. J. R. F. da Silva and R. J. P. Williams, *Biological Chemistry of the Elements: Inorganic Chemistry of Life*, Oxford, 1991; E. I. Solomon, M. D. Baldwin and M. D. Lowery, *Chem. Rev.*, 1992, **92**, 521.
- 2 R. Mukhopadhyay, S. Bhattacharjee and R. Bhattacharya, *J. Chem. Soc., Dalton Trans.*, 1994, 2799.
- 3 S. Brooker and V. McKee, *J. Chem. Soc., Dalton Trans.*, 1990, 2397.
- 4 M. G. B. Drew, O. W. Howarth, G. G. Morgan and J. Nelson, *J. Chem. Soc., Dalton Trans.*, 1994, 3149.
- 5 M. G. B. Drew, O. W. Howarth, C. J. Harding, N. Martin and J. Nelson, *J. Chem. Soc., Chem. Commun.*, 1995, 903.
- 6 C. J. Harding, J. Nelson and G. G. Morgan, work in progress.
- 7 M. A. Flanders and E. C. Lingafelter, *Inorg. Chem.*, 1976, **15**, 750.
- 8 (a) R. M. Kirchner, C. Mealli, M. Bailey, N. Howe, L. P. Torre, L. J. Wilson, L. C. Andrews, N. J. Rose and E. C. Lingafelter, *Coord. Chem. Rev.*, 1987, **77**, 89; (b) A. A. Balal, P. Chauduri, I. Fallis, L. J. Farrugia, R. Hartung, N. M. Macdonald, B. Nuber, R. D. Peacock, J. Weiss and K. Wieghardt, *Inorg. Chem.*, 1991, **30**, 4397.
- 9 S. K. Chandra and A. Chakravorty, *Inorg. Chem.*, 1991, 3795.
- 10 G. G. Morgan, PhD Thesis, Open University, 1995.
- 11 M. McCann, M. Casey, G. G. Morgan and J. Nelson, manuscript in preparation.
- 12 K. Wieghardt, *Angew. Chem., Int. Ed. Engl.*, 1994, **33**, 725.
- 13 G. M. Sheldrick, *Acta Crystallogr., Sect. A*, 1990, **46**, 467.
- 14 G. M. Sheldrick, SHELXL-93, program for crystal structure refinement, University of Göttingen.